pISSN 2288-6982 | eISSN 2288-7105

BIO DESIGN

MINI REVIEW P 47-54

# Structure-based drug discovery using NMR spectroscopy

**Ji-Hye Yun and Weontae Lee***
Department of Biochemistry, College Life Science and Biotechnology, Yonsei University, Seoul 120-749, Korea.
*Correspondence: wlee@spin.yonsei.ac.kr

**The structural information of biomolecules is essential for novel drug discovery. Recently, several new high-throughput drug-screening methods have been established. Nuclear magnetic resonance (NMR) spectroscopy is one of the most powerful techniques for drug development, providing critical information on molecular interactions for drug design in solution. Knowledge of the 3D structure and dynamic properties of drug target molecules is mandatory in performing initial hit selection and lead optimization. For this purpose, NMR spectroscopy has been developed and widely used. In particular, NMR is ideal for the fragment-based drug discovery (FBDD) strategy, because molecular interactions between target proteins and small ligands can be quickly identified at the atomic level. In this review, NMR techniques used for structure-based drug design will be discussed together with practical examples.**

## INTRODUCTION

In the past, many drugs were introduced due to accidental discoveries. During the 20$^{th}$ century, research fields such as genomics and proteomics were on the rise fueled by some events such as DNA structure determination (1950's), recombinant DNA technologies (1970's), and thereafter the structural information of biomolecules as well as knowledge on cellular signaling cascades and metabolic pathways have been accumulated and used for novel drug discovery and drug validation.

This led to the development of effective new drugs. Recently, fragment-based screening methods have been introduced rather than conventional high-throughput screening (HTS) methods of small molecules because of their advantages (e.g., compound size, higher hit rate, etc.). The drug discovery using fragment-based screening techniques consists of several steps: target selection, validation, lead identification, and optimization (Figure 1). Nuclear magnetic resonance (NMR) spectroscopy is a powerful technique for fragment-based drug discovery (FBDD), because it allows for easy identification of molecular interactions between target proteins and small ligands at the atomic level (Wishart, 2005; Lepre et al., 2004). The concept of NMR screening originated from chemical shift perturbation due to molecular interactions between receptor molecules and ligands observed in NMR experiments. Several examples utilizing NMR-based drug discovery such as development of Hsp90 inhibitor for the cancer treatment (Murray et al., 2010), optimization of BACE-1 (β-Site APP Cleaving Enzyme 1) inhibitors for the treatment of Alzheimer's disease (Wang et al., 2010), identification of novel inhibitor binding site of HIV-1 capsid protein for anti-viral drugs design (Goudreau et al., 2013) have been reported.

The NMR-based FBDD technique (Rees et al., 2004; Pellecchia et al., 2002) consists of two steps: 1) target-based screening and 2) ligand-based screening. In target-based screening, NMR titration experiments can be performed for chemical shift mapping to monitor the binding site of the target molecule upon ligand binding. For this purpose, target proteins of interest are labeled with stable isotopes ($^{15}N$ and $^{13}C$), and NH/C$^{\alpha}$H cross-correlation peaks on the 2D heteronuclear single-quantum coherence (HSQC) spectrum of proteins are analyzed with complete assignment of resonances. In the presence of ligand molecules, chemical shift perturbation data provides information on the ligand binding sites of the receptor molecule. Thereafter, this information is directly used to determine the 3D structure of the protein–ligand complex in solution by NMR spectroscopy. In addition, the dynamic properties of the protein are closely related to biological function via conformational transition. Although X-ray crystallography is powerful for determining the protein–ligand complex, it is limited in its ability to explain protein dynamics and weak binding. NMR spectroscopy is a useful tool to figure out protein dynamics, which is important considerations in drug discovery process.

For ligand-based screening, NMR experiments on saturation transfer difference (STD), transferred NOE (tr-NOE), diffusion coefficient measurement, and relaxation parameters (e.g., $T_1$, $T_2$) (Hajduk et al., 1997; Lin et al., 1997) have been used to identify lead compounds in a high-throughput manner. If a ligand molecule binds to its receptor, it exhibits line broadening of NMR resonances due to spin relaxation and the diffusion effect (Figure 2). In this review, several NMR techniques are described mainly focusing on two topics regarding structure determination and characterization of protein-ligand interaction.

## ISOTOPE LABELING OF TARGET PROTEINS

Most drug target molecules have a high molecular weight (i.e.,



 © 2014 Bio Design 

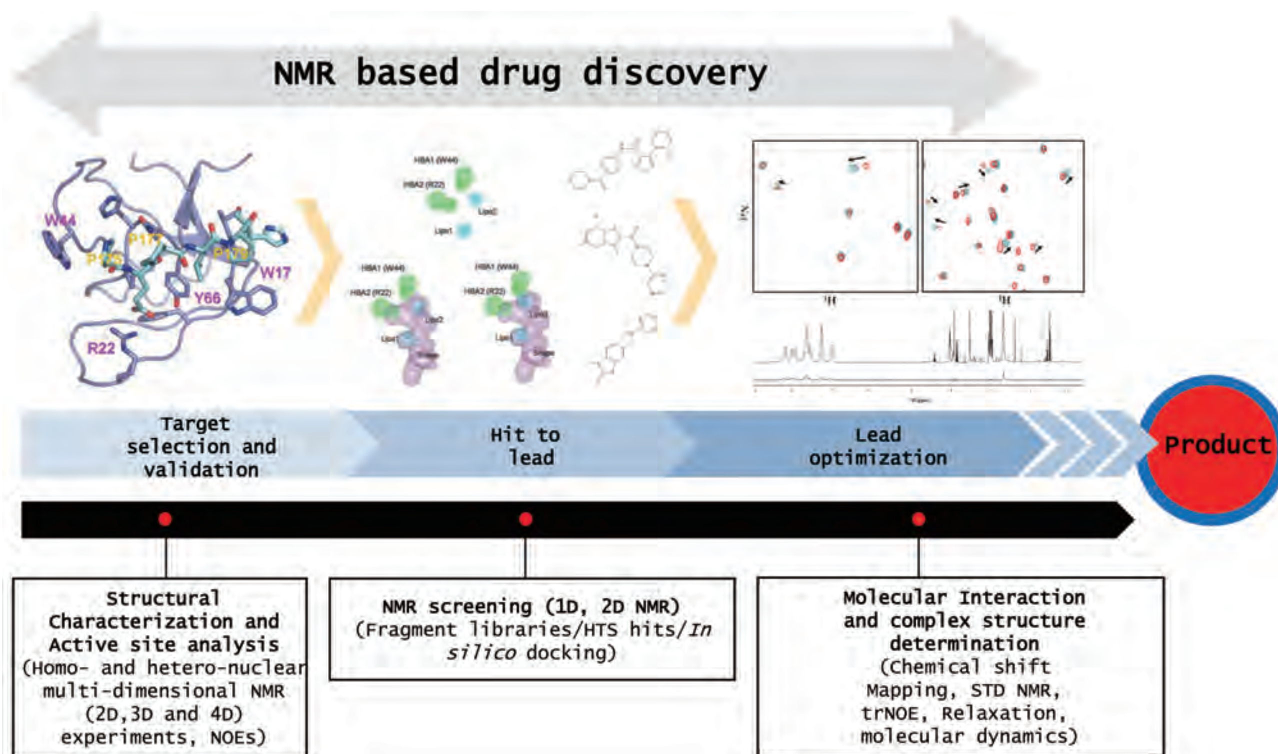


**FIGURE 1 | Schematic diagram for NMR-based drug discovery.** NMR spectroscopy is applicable to each stage during development.

above 10 KDa). In structure determination using conventional NMR techniques, the size limitation is a bottleneck because of the signal complexity and line broadening of NMR signals. Therefore, in many cases, a domain-specific method, which reconstructs the active domain from the full protein, or TROSY-based NMR methods are used (Pervushin et al., 1997). In addition, the isotope-labeling method (uniform $^{13}C/^{15}N$ labeling), selective amino acid labeling, and deuterium ($^{2}H$) labeling can help to resolve the signal complexity through multi-dimensional (3D and/or 4D) NMR experiments. For the stable isotope labeling of target molecules, the most common expression systems are bacterial systems, such as *E. coli* and yeast cells. In most cases, the uniform labeling of $^{13}C$ and $^{15}N$ is ample and efficient, though selective isotope labeling (Tong et al., 2008) is often used. Minimal media containing a $^{15}NH_4Cl$ or $^{13}C$-glucose source are used for bacteria cell cultures, and proteins are isotope-labeled when they are overexpressed by an inducer. Macromolecules could have poor NMR sensitivity due to rapid relaxation (Figure 2). To overcome the sensitivity problem, the deuterium-labeling method improves the sensitivity of NMR signals dramatically by decreasing both the relaxation rate and line width. A schematic diagram of the isotope-labeling technique of proteins for heteronuclear NMR experiments is shown in Figure 3A (Kim et al., 2011). NMR signals of large proteins with high molecular weights (>20 kDa) are greatly enhanced by $^{2}H/^{13}C/^{15}N$ isotope labeling combined with

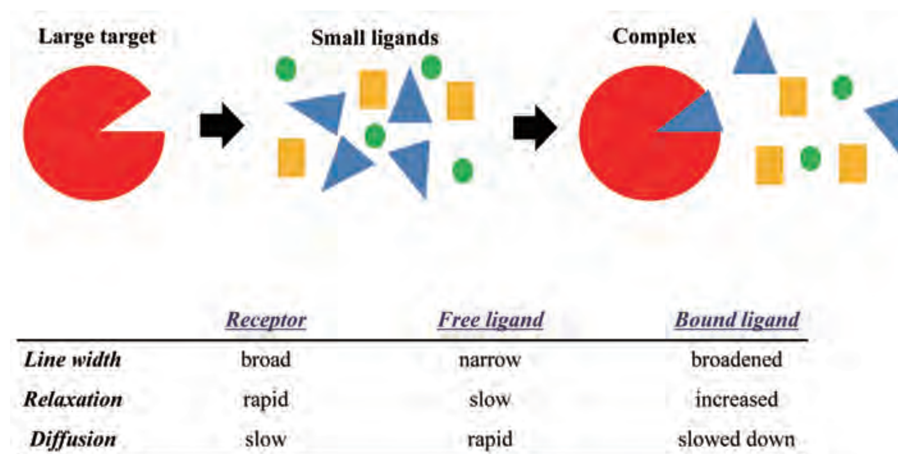


| | Receptor | Free ligand | Bound ligand |
|---|---|---|---|
| Line width | broad | narrow | broadened |
| Relaxation | rapid | slow | increased |
| Diffusion | slow | rapid | slowed down |

**FIGURE 2 | Principle of NMR signals upon receptor binding.** Different physical properties (relaxation and diffusion) modulate NMR signals of receptor and ligand molecules.

 © 2014 Bio Design 

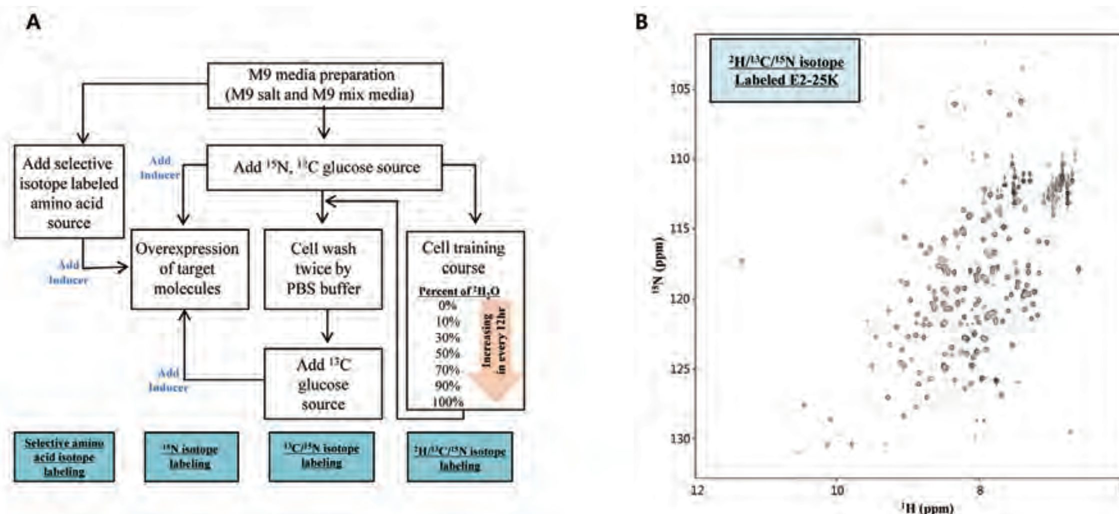


**FIGURE 3 | Flowchart of isotope-labeling strategy and NMR spectrum of triple-labeled ($^2H/^{13}C/^{15}N$) protein sample.** (A) For deuterium-labeling process, it is essential to train cells for different deuterium concentrations. (B) 2D TROSY-based $^1H$-$^{15}N$ HSQC spectrum of $^2H/^{13}C/^{15}N$ labeling protein. NMR experiment was performed in mixture of 90% $H_2O$ and 10% $2H_2O$ NMR buffer (50 mM $NaPO_4$, 100 mM NaCl, 2 mM DTT, and pH 7.0) at 298 K on a Bruker DRX 900 MHz equipped with a CryoProbe™ system.

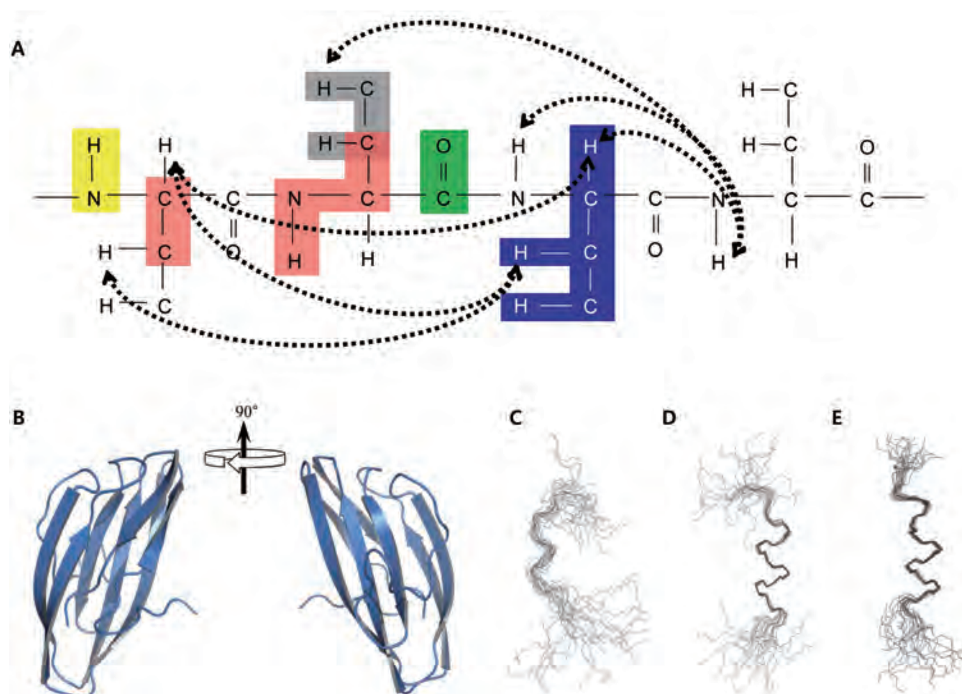


**FIGURE 4 | Schematic diagram of NMR assignment and solution structures calculated by NMR data.** (A) Diagram of backbone and side-chain assignments together with NOEs. Red, yellow, and green boxes indicate bond connections that can be detected by HNCACB, HSQC, and HNCO experiments, respectively. Gray and blue boxes indicate bond connections of side-chain atoms that can be observed in COSY and TOCSY experiments. Dotted lines represent NOEs by NOESY experiment. (B) Ribbon diagram of C-terminal regulatory domain of vEP as an example of structure determined by heteronuclear 2D and 3D NMR experiments. Superimposition of 20 energy-minimized structures of FTZ-F1 in $H_2O$ (C), in TFE (D), and in the presence FTZ-F1 LBD as an example of structures determined by homonuclear 2D NMR experiments.

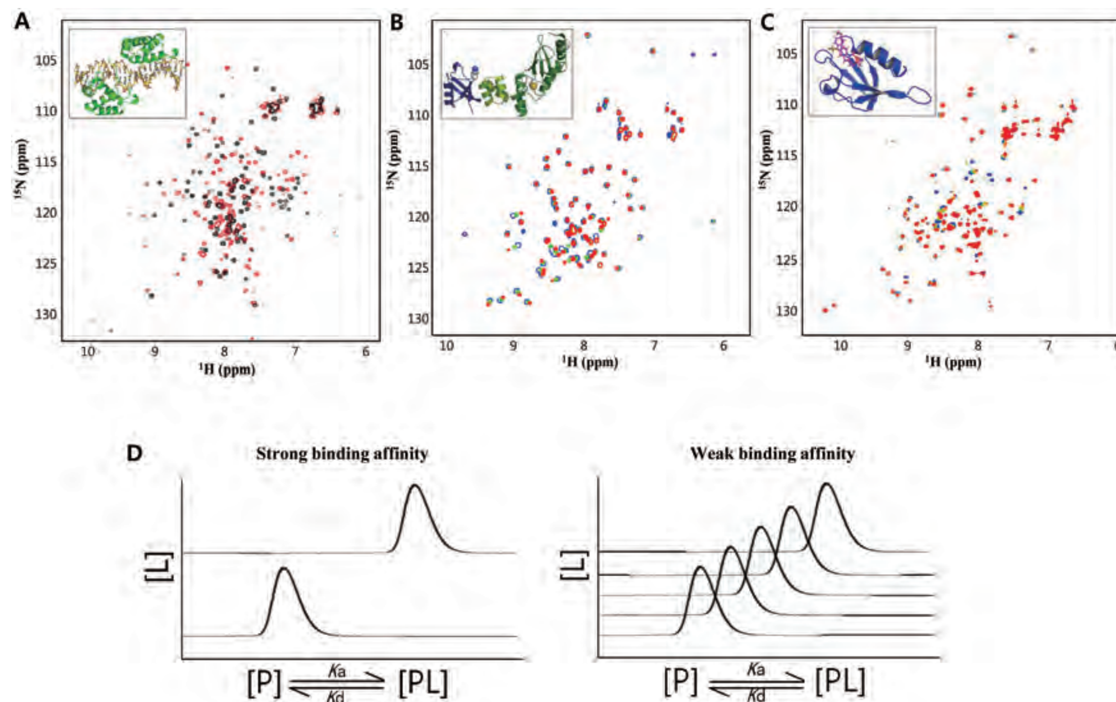


**FIGURE 5 | $^{1}$H-$^{15}$N HSQC spectra of protein–DNA, protein–protein, and protein–inhibitor complexes for chemical shift mapping.** (A) NMR resonances of backbone atoms of protein were perturbed upon DNA binding. (B) Protein resonances were shifted upon partner protein binding. (C) Chemical shift perturbations were monitored upon inhibitor binding. (D) Schematic diagram representing signal properties caused by strong (left) and weak (right) binding affinity during molecular interaction. In strong binding affinity, significant peak shift of protein between free and ligand-bound state can be observed, whereas stepwise peak shift is observed in weak binding affinity.

TROSY-based NMR experiments. As an example, Figure 3B demonstrates the quality of the 2D TROSY-HSQC spectrum of a $^{2}$H/$^{13}$C/$^{15}$N labelled 25kDa protein (Ko et al., 2010).

## HETERONUCLEAR NMR EXPERIMENTS AND STRUCTURE CALCULATION OF PROTEINS

Isotope-labeled proteins are directly applicable to heteronuclear 2D and 3D NMR experiments. Backbone resonances can be assigned by triple-resonance NMR experiments (e.g., HNCACB, CBCA(CO)NH, HNCA, HNCO) (Figure 4A) (Vuister et al., 1993; Grzesiek et al., 1992; Stonehouse et al., 1995; Muhandiram et al., 1994; Ikura et al., 1990; Grzesiek et al., 1993). J-coupling-derived dihedral angle restraints for secondary structure information are obtained experimentally from the results of backbone resonance assignments. Side-chain chemical shifts are assigned by data from HBHA(CO)NH, HCC(CO)NH, (H)CC(CO)NH, HCCH-total correlation spectroscopy (TOCSY) and $^{15}$N-edited TOCSY experiments (Figure 4A) (Kay et al., 1993; Bax et al., 1985a). Nuclear Overhauser effect (NOE)-derived inter- and intra-molecular distance restraints are collected by analysis of amide, aliphatic, and aromatic NOEs from nuclear Overhauser and exchange spectroscopy (NOESY) spectra (e.g., $^{15}$N-edited NOESY, $^{13}$C-edited NOESY) (Davis et al., 1992; Bax et al., 1985a). For structure calculations, the CYANA (Guntert, 2004), CNS (Brunger et al., 1998), and XPLOR (Schweiters et al., 2006) programs are used. The final structures with the lowest energy are validated by common validation tools. The most popular and widely used program is the PROCHECK program (Laskowski et al., 1996). Figure 4B demonstrates the solution structure calculated using data from NMR experiments. As an example, the structure of the C-terminal regulatory domain of extracellular metalloprotease derived from *vibrio vulnificus* has been determined for developing antimicrobial drugs related to fatal septicemia (Yun et al., 2012a; Yun et al., 2013a).

## HOMONUCLEAR NMR EXPERIMENTS AND STRUCTURE CALCULATION OF LIGANDS

It is possible to determine the structure of peptide ligands and small organic compounds through homonuclear 2D NMR experiments (e.g., double quantum filtered-correlation spectroscopy (DQF-COSY), 2D TOCSY, and 2D NOESY). For organic compounds, HMQC and HMBC experiments are used to assign resonances using natural abundant $^{13}$C signals. Carbon and proton resonances are identified by correlation peaks under bond connections through the combined techniques of HMQC, HMBC, DQF-COSY, and $^{1}$H-$^{1}$H TOCSY (Rance et al., 1983; Bax et al., 1986a; Bax et al., 1985a; Bax et al., 1983; Bax et al., 1986b; Schleucher et al., 1994; Lim et al., 2001). 2D NOESY experiments provide inter- and intra-molecular NOEs based on cross-peak intensities for structure information including stereochemistry

 © 2014 Bio Design 

of compounds. We have determined the structure of a novel pheromone daumone secreted from *Caenorhabditis elegans* having a regulatory role in chemosensory processes during ageing and development. We demonstrated how the molecular structure of natural daumone isolated from C. *elegans* could be determined by NMR spectroscopy (Jeong et al., 2005). Figure 4C, 4D, and 4E represent three solution structures of the FTZ-f1 cofactor peptide in different environments (Yun et al., 2012b).

## CHEMICAL SHIFT MAPPING

Chemical shift perturbation experiments are one of the most widely used NMR techniques to determine the interaction site between a protein and ligand molecule (Peng et al., 2004). Upon ligand titration, chemical shift perturbations indicating binding surface of the receptor protein are observed in the 2D $^{1}H$-$^{15}N$ HSQC spectra. However, it may also reflect the conformation change of protein as a result of ligand binding. To calculate the average values of chemical shift perturbation, the following equation is used: $\Delta\delta_{AV} = ((\Delta\delta_{1H})^2 + (0.2 \times \Delta\delta_{15N})^2)^{1/2}$ Here, $\Delta\delta_{AV}$, $\Delta\delta_{1H}$, and $\Delta\delta_{15N}$ indicate the average, $^{1}H$, and $^{15}N$ chemical shift changes, respectively. Examples of chemical shift mapping by NMR are shown in Figure 5: protein–DNA (Figure 5A) (Moon et al., 2014; Lee et al., 2012; Ko et al., 2009; Ko et al., 2008; Sung et al., 2014), protein–protein (Figure 5B) (Ko et al., 2009a; Yun et al., 2013b), and protein–chemical ligand (Figure 5C) (unpublished). If the binding affinity between the DNA binding protein (transcription factor) and the DNA is strong compared with the protein–protein or protein–chemical binding affinity, the chemical shift perturbation is significant upon DNA titration because of the slow exchange mode (Figures 5A and 5D). In contrast, stepwise chemical shift changes are detectable in weak binding affinity cases (Figures 5B, 5C, and 5D). In the fast exchange mode, the dissociation constant ($K_d$) could also be measured.

## PROTEIN DYNAMICS

The dynamic properties of proteins are closely related to their functions and molecular interactions with other molecules. NMR spectroscopy has the power to provide protein dynamicity and flexibility in the solution state. $T_1$, $T_2$, and heteronuclear NOE (XNOE) experiments (Farrow et al., 1994; Grzesiek et al., 1993) are used to analyze the dynamic properties of $^{15}N$, $^{13}C$, or $^{2}H$ nuclei on proteins (Jarymowycz et al., 2006). Generally, $T_1$, $T_2$, and heteronuclear NOE (XNOE) experiments are good method to analyze protein dynamics easily, however there are still some sensitivity issues regarding fast signal decay. The longitudinal ($R_1$) and transverse ($R_2$) relaxation rates are obtained via several relaxation delay times. Upon ligand binding, the spin relaxation rates change, representing the degree of local protein mobility. The heteronuclear cross-relaxation rate can be measured from XNOE experiments. Order parameters ($S_2$) and exchange rates ($R_{ex}$) are further calculated using data from spin relaxation experiments. Other parameters to confirm protein–ligand interactions are the transferred residual dipolar coupling (Bolon et al., 1999) and transferred cross-correlated relaxation (Carlomagno et al., 1999) in terms of interacting geometries. Our previous studies described how backbone dynamics were

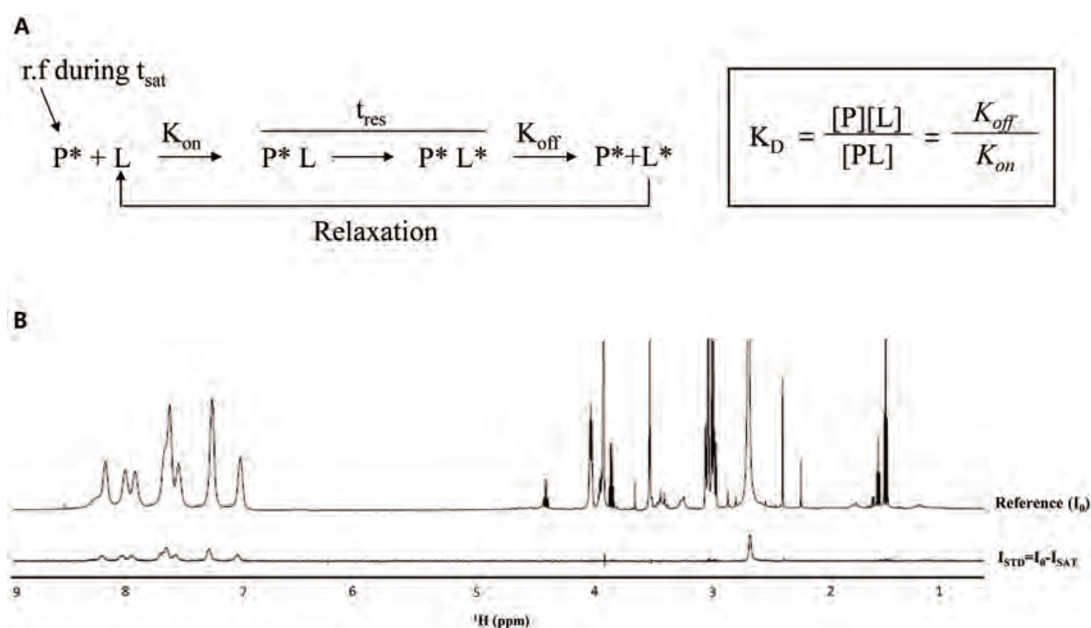


**FIGURE 6 | Scheme of saturation transfer difference (STD) NMR experiment.** (A) Simplified theory of intermolecular magnetization transfer from saturated protein to bound ligand during saturation time ($t_{sat}$). (B) STD-NMR spectrum recorded by selective saturation pulse. Proton 1D NMR spectrum without protein saturation (off-resonance) is reference spectrum ($I_0$). STD spectrum ($I_{STD}$) is obtained by subtracting on-resonance from off-resonance ($I_{STD}$=I0-$I_{SAT}$). STD spectrum ($I_{STD}$) reflects binding site of ligand in receptor-bound state.

measured and analyzed to elucidate protein function and ligand interaction (Hong et al., 2004; Yun et al., 2013a; Yun et al., 2013b; Jeong et al., 2013).

## SATURATION TRANSFER DIFFERENCE (STD) NMR

STD NMR spectroscopy is frequently used for ligand-based screening. Information on receptor–ligand interactions is critical for designing lead compounds or antagonists. STD-NMR originated from NOE, and the resonance signals of ligand molecules in both free and receptor-bound states are modulated by spin diffusion effects (Begley et al., 2013; Ludwig et al., 2009). Therefore, STD-NMR has the advantage of providing ligand information without NMR data of the receptor molecule. For optimum STD-NMR experiments, one of the most important factors is the off-rate ($K_{off}$) in the receptor–ligand complex. If the binding affinity of the ligand is weak, a strong STD-NMR signal that relies on a higher $K_{off}$ rate can be observed. In contrast, there are no detectable STD signals for the strong binding of the ligand depending on a low $K_{off}$ rate. The range of $K_d$ for STD-NMR experiments is between $10^{-8}$ M and $10^{-3}$ M (Figure 6A). In addition, the selective saturation pulse, which selectively irradiates protein resonances, is an important factor. The STD spectrum ($I_{STD}$) is obtained by subtracting on-resonance ($I_{SAT}$) from off-resonance ($I_0$) (Figure 6B). The STD spectrum ($I_{STD}$) provides the interaction site of the ligand molecule upon receptor binding. For big macromolecules, the inherent poor spatial proton density generates poor sensitivity in STD-NMR. This problem can be solved by waterLOGSY experiments, which enhance the sensitivity of STD signals using magnetization transfer from bulk water to the ligand through the receptor (Dalvit et al., 2001).

## TRANSFERRED-NOE (TR-NOE) EXPERIMENT

NOE provides information on the inter-nuclear distance ($r^6$) between two nuclei spins having both inter- and intra-molecular magnetization transfers (Lucas et al., 2003; Feng., 1994; Jung et al., 2000). Tr-NOE experiment is very useful method for obtaining information on the bound state ligand even though dissociation constants limitations (1mM and 10nM) are existed. As compare as STD-NMR, both the free and bound states of ligand molecules can be observed in tr-NOE experiment. The intensity of tr-NOEs depends on the ligand to protein ratio, and strong tr-NOE signals can be measured for the maximum molecular ratio of the receptor–ligand complex. The observation of tr-NOE signals comes from the correlation time ($\tau_c$) of the free and bound ligands. Small molecules have short correlation times and positive NOEs, whereas receptor-bound ligands exhibit behavior similar to that of macromolecules, showing strong negative NOEs (tr-NOEs) (Figure 7A). From tr-NOE experiments, the inter-molecular interactions between the ligand and receptor molecule are readily identified, which provides structural information on the bound ligand in solution. The transferred NOESY experiment is a very useful technique to determine the binding capability of a ligand molecule combining with STD-NMR. An example of tr-NOE data for a ligand–protein interaction is shown in Figure 7B. The structure of the protein–ligand complex could be generated by data from tr-NOE experiments (Figure 7C), and this information is essential for designing novel ligands or inhibitor molecules (Ko et al., 2009a).

## TRANSFERRED CROSS SATURATION (TCS)

As compare with STD and tr-NOE experiment, transferred cross

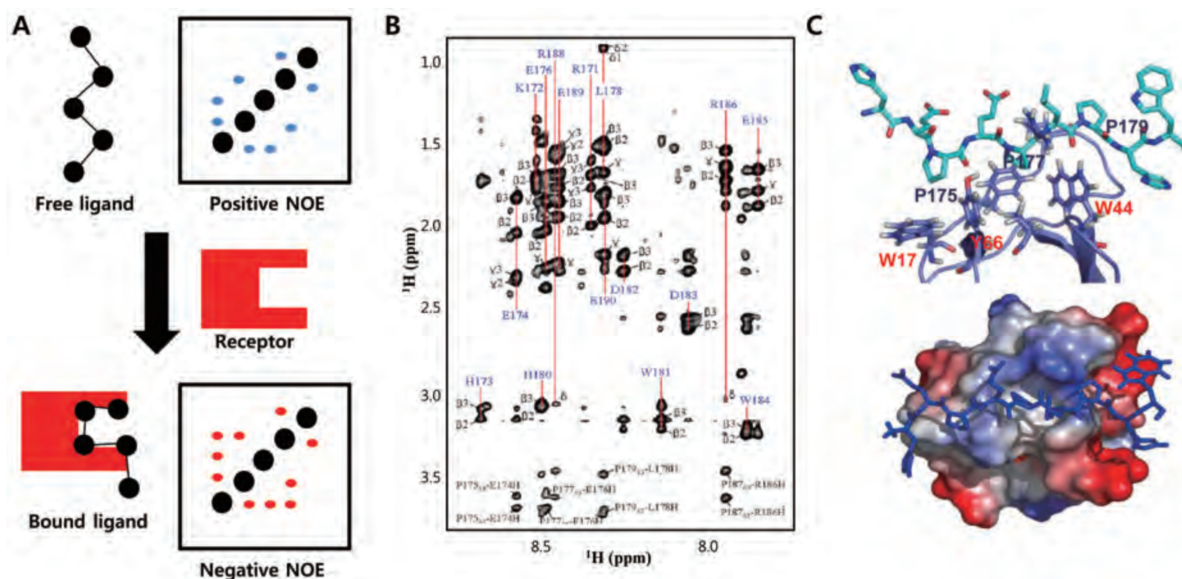


**FIGURE 7 | Demonstration of transferred NOE (tr-NOE) experiment and example of tr-NOEs.** (A) Schematic diagram of tr-NOE data shows NMR signals of both free and bound ligands. (B) NOESY spectrum representing tr-NOEs between backbone NH and side-chain proton resonances. (C) NMR structure of protein–peptide ligand complex built using data from tr-NOEs.

 © 2014 Bio Design 

saturation (TCS) experiment is proper method for identifying binding residues of protein ligands, which makes complexes with macromolecules such as membrane protein (Matsumoto et al., 2010). The efficiency of TCS depends on several experimental factors such as binding constants, molar ratio and molecular weights between the ligands and the receptors. In general, excess amount of U-$^{2}H$, $^{15}N$ labeled protein ligands and non-labeled receptor protein are mixed together in 10% $H_2O$/90% $D_2O$ for the TCS. Aliphatic protons located in the receptor protein are saturated by radio-frequency (RF) - irradiation. By spin diffusion, the saturation of aliphatic protons on receptor protein transfer to the protons in the protein ligands forming complexes with receptor proteins. In 2D-HSQC spectra, ligand protons interacting with receptor protein reveal large signal reduction, and it can be used for the calculation of signal intensity ratio.

## CONCLUSION

NMR spectroscopy is an extremely powerful analytical technique in modern drug development. NMR-based drug discovery enables the application of FBDD for developing molecular interaction inhibitors. NMR allows structure determination in the solution state and provides dynamic properties of the target molecule. The ligand or partner protein-binding sites of the receptor can be identified and validated using the chemical shift mapping technique. STD-NMR is useful for ligand-based screening, providing information on receptor–ligand interactions critical for designing inhibitor molecules. NMR spectroscopy can also be used with HTS, which is mandatory in modern drug discovery. In conclusion, since NMR spectroscopy is an essential technique with many advantages over X-ray crystallography and molecular modeling methods in the drug-development process, it could be made even more powerful by combining it with other methods.

### ACKNOWLEDGEMENTS

This work was supported by the National Research Foundation of Korea (NRF) grant funded by the Korea government (MEST) (NRF-2013R1A2A2A01068963) and in part by Brain Korea Plus (BK+) project.

### AUTHOR INFORMATION

The authors declare no potential conflicts of interest.

Original Submission: April 29, 2014
Revised Version Received: May 27, 2014
Accepted: May 28, 2014

### REFERENCES

Bax, A., and Davis, D.G. (1985a). MLEV-17-based two-dimensional homonuclear magnetization transfer spectroscopy. *J Magn Reson* **65**, 355–360.

Bax, A., and Davis, D.G. (1985b). Practical aspects of two-dimensional transverse NOE spectroscopy. *J Magn Reson* **63**, 207–213.

Bax, A., Griffey, R.H., and Hawkins, B.L. (1983). Correlation of proton and nitrogen-15 chemical shifts by multiple quantum NMR. *J Magn Reson* **55**, 301–315.

Bax, A., and Subramanian, S. (1986a). Sensitivity-enhanced two-dimensional heteronuclear shift correlation NMR spectroscopy. *J Magn Reson* **67**, 565–570.

Bax, A., and Summers, M.F. (1986b). $^{1}H$ and $^{13}C$ assignments from sensitivity enhanced detection of heteronuclear multiple-bond connectivity by two-dimensional multiple quantum NMR. *J Am Chem Soc* **108**, 2093–2094.

Begley, D.W., Moen, S.O., Pierce, P.G., and Zartler, E.R. (2013). Saturation transfer difference NMR for fragment screening. *Curr Protoc Chem Biol* **5**, 251–268.

Bolon, P.J., Al-Hashimi, H. M., and Prestegard, J.H. (1999). Residual dipolar coupling derived orientational constrains on ligand geometry in a 53Kda ligand–protein complex. *J Mol Biol* **293**, 107–115.

Brunger, A.T., Adams, P.D., Clore, G.M., DeLano, W.L., Gros, P., Grosse-Kunstleve, R.W., Jiang, J.-S., Kuszewski, K., Nilges, M., Pannu, N.S., Read, R.J., Rice, L.M., Simonson, T., and Warren, G.L. (1998). Crystallography & NMR system: a new software suite for macromolecular structure determination. *Acta Crystallogr* **54**, 905-921.

Carlomagno, T., Felli, I.C., Czech, M., Fischer, R., Sprinzl, M., and Griesinger, C. (1999). Transferred cross-correlated relaxation: application to the determination of Sgar Puker in an aminoacylated tRNA Mimetic weakly bound to EF-Tu. *J Am Chem Soc* **121**, 1945–1948.

Dalvit, C., Fogliatto, G.P., Stewart, A., Veronesi, M., and Stockman, B. (2001). WaterLOGSY as a method for primary NMR screening: Practical aspects and range of applicability. *J Biomol NMR* **21**, 349–359.

Davis, A.L., Keeler, J., Laue, E.D., and Moskau, D. (1992). Experiments for recording pure-absorption heteronuclear correlation spectra using pulsed field gradients. *J Magn Reson* **98**, 207–216.

Farrow, N.A., Muhandiram, R., Singer, A.U., Pascal, S.M., Kay, C.M., Gish, G., Shoelson, S.E., Pawson, T., Forman-Kay, J.D., and Kay, L.E. (1994). Backbone dynamics of a free and a phosphopeptide-complexed Src homology 2 domain studied by $^{15}N$ NMR relaxation. *Biochemistry* **33**, 5984–6003.

Feng, N. (1994). Recent developments in transferred NOE methods. *Prog NMR Spectrosc* **26**, 517–606.

Goudreau, N., Lemke, C.T., Faucher, A.M., Grand-Maitre, C., Goulet, S., Lacoste, J.E., Rancourt, J., Malenfant, E., Mercier, J.F., Titolo, S., and Mason, S.W. (2013). Novel inhibitor binding site discovery on HIV-1 capsid N-terminal domain by NMR and X-ray crystallography. *ACS Chem Biol* **8**, 1074–1082.

Guntert, P. (2004). Automated NMR structure calculation with CYANA. *Methods Mol Biol* **278**, 353–378.

Grzesiek, A., and Bax, A. (1993). The origin and removal of artifacts in 3D HCACO spectra of proteins uniformly enriched with 13C. *J Magn Reson* **102**, 103–106.

Grzesiek, S., and Bax, A. (1992). Improved 3D triple resonance NMR techniques applied to a 31 kDa protein. *J Magn Reson* **96**, 32-440.

Grzesiek, S., and Bax, A. (1993). The importance of not saturating $H_2O$ in protein NMR. Application to sensitivity enhancement and NOE measurements. *J Am Chem Soc* **115**, 12593-12594.

Hajduk, P.J. Olejniczak, E.T., and Fesik, S.W. (1997). One-dimensional relaxation- and diffusion-edited NMR methods for screening compounds that bind to macromolecules. *J Am Chem Soc* **119**, 12257–12261.

Ikura, M., Kay, L.E., and Bax, A. (1990). A novel approach for sequential assignment of proton, carbon-13, and nitrogen-15 spectra of larger proteins: heteronuclear triple-resonance three-dimensional NMR spectroscopy. Application to calmodulin. *Biochemistry* **29**, 4659–4667.

Jarymowycz, V., and Stone, M.J. (2006). Fast time scale dynamics of protein backbone: NMR relaxation methods applicaiton, and functional consequences. *Chem Rev* **106**, 1624–1671.

Jeong, K.W., Ko, H., Lee, S.A., Hong, E., Ko, S., Cho, H.S., Lee, W., and Kim, Y. (2013). Backbone Dynamics of an Atypical Orphan Response Regulator Protein, Helicobacter pylori 1043. *Mol Cells* **35**, 158–165.

Jeong, P.Y., Jung, M., Yim, Y.H., Kim, H., Park, M., Hong, E., Lee, W., Kim, Y.H., Kim, K., and Paik, Y.K. (2005). Chemical structure and biological activity of the Caenorhabditis elegans dauer-inducing pheromone. *Nature* **433**, 541–545.

Jung, J.W., An, J.H., Na, K.B., Kim, Y.S., and Lee, W. (2000). Active Site

and Substrate Binding Mode of Malonyl-CoA Synthetase Determined by Transfered Nuclear Overhauser Effect Spectroscopy, Site Directed Mutagenesis and Comparative Modeling Studies. *Protein Sci*. **9**,1294–1303.

Kay, L.E., Xu, G.Y., Singer, A.U., Muhandiram, D.R., and Forman-Kay, J.D. (1993). A gradient-enhanced HCCH TOCSY experiment for recording side-chain H-1 and C-13 correlations in H2O samples of proteins. *J Magn Reson* **101**, 333–337.

Kim, H., Hong, E., and Lee, W. (2011). Cost-effective isotope labeling technique developed for 15N/13C-labeled proteins. *Journal of the Korean Magnetic Resonance Society* **15**, 115–127.

Ko, S., Ahn, K.E., Lee, Y.M., Ahn, H.C., and Lee, W. (2009a). Structural Basis of the Auto-inhibition Mechanism of Nonreceptor Tyrosine Kinase PTK6. *Biochem Biophy Res Com* **48**, 827–838.

Ko, S., Kang, G.B., Song, S.M., Sheng, Y., Cheong, C., Jung, Y.K., Arrowsmith, C.H., Avvakumov, G.V., Dhe-Paganon, S., Yoo, Y.J., Eom, S.H., and Lee, W. (2010). Structural basis of E2-25K/UBB$^{+1}$ interaction leading to proteasome inhibition and neurotoxicity in Alzheimer's disease. *J Biol Chem* **285**, 36070–36080.

Ko, S., Jun, S.H., Bae, H., Byun, J.S., Han, W., Park, H., Yang, S.W., Park, S.Y., Jeon, Y.H., Cheong, C., Kim, W.T., Lee, W. and Cho, H.S. (2008). Structure of the DNA-binding domain of NgTRF1 reveals unique features of plant telomere-binding proteins. *Nucleic Acids Res* **36**, 2739–2755.

Ko, S., Yu, E.Y., Shin, J., Yoo, H.H., Tanaka, T., Kim, W.T., Cho, H.S., Lee, W., and Chung, I.K. (2009b). Solution structure of the DNA binding domain of rice telomere binding protein RTBP1. *Biochemistry* **48**, 827–838.

Laskowski, R.A., Rullmannn, J.A., MacArthur, M.W., Kaptein, R., and Thornton, J.M. (1996). AQUA and PROCHECK-NMR: programs for checking the quality of protein structures solved by NMR. *J Biomol NMR* **8**, 477-486.

Lee, W.K., Yun, J.H., Lee, W., and Cho, M.H. (2012). DNA-Binding Domain of AtTRB2 Reveals Unique Features of a Single Myb Histone Protein Family that Binds to Both Arabidopsis- and Human-Type Telomeric DNA Sequences. *Molecular Plant* **5**, 1406–1408.

Lepre, C.A., Moore, J.M., and Peng, J.W. (2004). Theory and applications of NMR-based screening in pharmaceutical research. *Chem Rev* **104**, 3641–3676.

Lim, S., Li, S.Z., Lee, C., Yoon, C.J., Baik, J.H., and Lee, W. (2001). Minimization of MC1R selectivity by modification of the core structure of a-MSH-ND. *Chem and Biol* **122**, 1–14.

Lin, M., Shapiro, M.J., and Wareing, J.R. (1997). Diffusion-edited NMR-affinity NMR for direct observation of molecular interactions. *J Am Chem Soc* **119**, 5249–5250.

Lucas, L.H., Yan, J., Larive, C.K., Zartler, E.R., and Shapiro, M.J. (2003). Transferred nuclear Overhauser effect in nuclear magnetic resonance Diffusion measurements of ligand–protein binding. *Anal Chem* **75**, 627–634.

Ludwig, C., Guenther, U.L. (2009). Ligand based NMR methods for drug discovery. *Front Biosci (Landmark Ed)* **14**, 4565–4574.

Moon, S., Lee, Y.W., Kim, W.T., and Lee, W. (2014). Solution structure of CEH-37 homeodomain of the nematode Caenorhabditis elegans. *Biochem Biophy Res Com* **443**, 370–375.

Matsumoto, M., Ueda, T., and Shimada, I. (2010). Theoretical analyses of the transferred cross-saturation method. *J Magn Reson* **205**, 114-124.

Muhandiram, D.R., and Kay, L.E. (1994). Gradient-enhanced triple-resonance three-dimensional NMR experiments with improved sensitivity. *J Magn Reson* **103**, 203-216.

Murray, C.W., Carr, M.G., Callaghan, O., Chessari, G., Congreve, M., Cowan, S., Coyle, J.E., Downham, R., Figueroa, E., Frederickson, M., Graham, B., McMenamin, R., O'Brien, M.A., Patel, S., Phillips, T.R., et al. (2010). Fragment-based drug discovery applied to Hsp90. Discovery of two lead series with high ligand efficiency. *J Med Chem* **53**, 5942–5955.

Pellecchia, M., Sem, D.S., and Wuthrich, K. (2002). NMR in drug discovery. *Nat Rev Drug Discov* **1**, 211–219.

Peng, C., Unger, S.W., Filipp, F.V., Sattler, M., and Szalma, S. (2004). Automated evaluation of chemical shift perturbation spectra: New approaches to quantitative analysis of receptor-ligand interaction NMR spectra. *J Biomol NMR* **29**, 491–504.

Pervushin, K., Riek, R., Wider, G., and Wuthrich, K. (1997). Attenuated T2 relaxation by mutual cancellation of dipole-dipole coupling and chemical shift anisotropy indicates an avenue to NMR structures of very large biological macromolecules in solution. *Proc Natl Acad Sci USA* **94**, 12366–12371.

Rance, M., Sorensen, O.W., Bodenhausen, G., Wagner, G., Ernst, R.R., and Wuthrich, K. (1983). Improved spectral resolution in cosy $^1$H NMR spectra of proteins via double quantum filtering. *Biochem Biophys Res Commun* **117**, 479–485.

Rees, D.C., Congreve, R., Murray, C.W., and Carr, R. (2004). Fragment-based lead discovery. *Nat Rev Drug Discov* **3**, 660–672.

Schleucher, J., Schwendinger, M., Sattler, M., Schmidt, P., Schedletzky, O., Glaser, S.J., Sorensen, O.W., and Griesinger, C. (1994). A general enhancement scheme in heteronuclear multidimensional NMR employing pulsed field gradients. *J Biomol NMR* **4**, 301–306.

Schweiters, C.D., Kuszewski, J.J., and Clore, G.M. (2006). Using Xplor-NIH for NMR molecular structure determination. *Progr NMR Spectroscopy* **48**, 47-62.

Stonehouse, J., Clowes, R.T., Shaw, G.L., Keeler, J., and Laue, E.D. (1995). Minimization of sensitivity losses due to the use of gradient pulses in triple-resonance NMR of proteins. *J Biomol NMR* **5**, 226–232.

Sung, H.J., Choi, S., Lee, J.W., Ok, C.Y., Bae, Y.S., Kim, Y.H., Lee, W., Heo K., and Kim, I.H. (2014). Inhibition of human neutrophil activity by an RNA aptamer bound to interleukin-8. *Biomaterials* **35**, 578–589.

Tong, K.I., Yamamoto, M., and Tanaka, T. (2008). A simple method for amino acid selective isotope labeling of recombinant proteins in E.coli. *J Biomol NMR* **42**, 59-67.

Vuister, G.W., and Bax, A. (1993). Quantitative J correlation: A new approach for measuring homonuclear three bond J(HNHa) coupling constants in 15N-enriched proteins. *J Am Chem Soc* **115**, 7772-7777.

Wang, Y.S., Strickland, C., Volqt, J.H., Kennedy, M.E., Beyer, B.M., Senior, M.M., Smith, E.M., Nechuta, T.L., Madison, V.S., Czarniecki, M., Mckittrick, B.A., Stamford, A.W., Parker, E.M., Hunter, J.C., Greenlee, W.J., et al. (2010). Application of fragment-based NMR screening, X-ray crystallography, structure-based design, and focused chemical library design to identify novel microM leads for the development of nM BACE-1 (beta-site APP cleaving enzyme 1) inhibitors. *J Med Chem* **53**, 942–950.

Wishart, D. (2005). NMR spectroscopy and protein structure determination: applications to drug discovery and development. *Curr Pharm Biotechnol* **6**, 105–120.

Yun, J.H., Kim, H., Park, J.E., Cheong, H.K., Cheong, C., Lee, J.S., and Lee, W. (2012a). $^1$H, $^{15}$N and $^{13}$C backbone assignments and secondary structures of C-ter100 domain of vibrio extracellular metalloprotease derived from vibrio vulnificus. *Bull Korean Chem Soc* **33**, 10.

Yun, J.H., Kim, H., Park, J.E., Lee, J.S., and Lee, W. (2013a). Solution structure and dynamics of C-terminal regulatory domain of a novel vibrio extracellular metalloprotease. *Biochem Biophy Res Com* **430**, 541–546.

Yun, J.H., Ko, S., Lee, C.K., Cheong, H.K., Cheong, C., Yoon, J.B., and Lee, W. (2013b). Solution Structure and Rpn1 Interaction of the UBL Domainof Human RNA Polymerase II C-terminal Domain Phosphatase. *PLOs one* **8**, 1–8.

Yun, J.H., Lee, C.J., Jung, J.W., and Lee, W. (2012b). Solution structure of LXXLL-related cofactor Peptide of orphan nuclear receptor FTZ-F1. *Bull Korean Chem Soc* **33**, 583–588.

 © 2014 Bio Design 